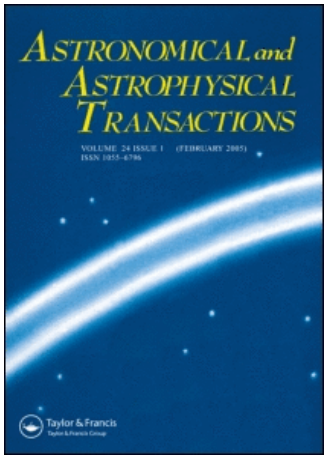

Astronomical & Astrophysical Transactions
The Journal of the Eurasian Astronomical Society
Publication details, including instructions for authors and subscription information:
http://www.informaworld.com/smpp/title~content=t713453505

RPAE calculations of the isoelectronic series **C**$^-$, **N** and **O** photoionization cross-sections

M. Ya. Amusiai [ab]; L. V. Chernysheva [b]
[a] A. F. Ioffe Physical-Technical Institute, St. Peterburg, Russia
[b] Institute of Physics and Astronomy, University of Aarhus, Aarhus, Denmark

Online Publication Date: 01 January 1997
To cite this Article: Amusiai, M. Ya. and Chernysheva, L. V. (1997) 'RPAE calculations of the isoelectronic series **C**$^-$, **N** and **O** photoionization cross-sections', Astronomical & Astrophysical Transactions, 12:2, 247 - 261
To link to this article: DOI: 10.1080/10556799708232081
URL: http://dx.doi.org/10.1080/10556799708232081

Astronomical and Astrophysical Transactions, 1997, Vol. 12, pp. 247–261
Reprints available directly from the publisher
Photocopying permitted by license only

RPAE CALCULATIONS OF THE ISOELECTRONIC SERIES C^-, N AND O^+ PHOTOIONIZATION CROSS-SECTIONS

M. Ya. AMUSIA[1,2] and L. V. CHERNYSHEVA[2]

[1] *A. F. Ioffe Physical-Technical Institute, St. Peterburg, Russia*
[2] *Institute of Physics and Astronomy, University of Aarhus, Aarhus, Denmark*

(Received November 30, 1995)

Calculations were performed for the isoelectronic series C^- ($Z = 6$), $N(Z = 7)$, O^+ ($Z = 8$) having for the same configuration $1s^2 2s^2 2p^3$. The spin-polarized version of the Hartree–Fock approximation (SPHF) was used in which each subshell is separated into two levels with opposite spin projections $1s^1\uparrow 1s^1\downarrow 2s^1\uparrow 2s^1\downarrow 2p^3\uparrow$. The estimations have demonstrated that corrections introduced by spin-polarized random phase approximatoin with exchange (SPRPAE) proved to be important. Therefore, the peculiarities of the cross-sectional behavior in the SPHF and the SPRPAE taking into account corrections in different transitions and simultaneously in all transitions were calculated. As expected abrupt variation of the cross-section from one atom to another took place: in the negative ion the main contribution is the continuous spectrum while in the neutral atom the contribution of discrete excitations is important, becoming the leading contribution for the positive ion. Because a simple inter- and extrapolation atomic cross-section behavior proved to be inadequate, a complete calculation for each chosen object is neccesary. Only the existence of a proper computer program allows us to perform SPHF and SPRPAE calculations of atomic photoionization cross-sections comparatively simply and effectivly.

KEY WORDS Atom, ion, photoionization, cross-section, oscillator strength, spin-polarised Hartree–Fork method, spin-polarised random phase approximation with exchange calculations

1 INTRODUCTION

Investigation of photoionization process in atoms and ions is of interest from different points of view. First, it is desirable to have data on the processes which very often take place in natural conditions. Such data are of importance not only in some scientific domains, for example, astrophysics and solid state physics but also in technological applications. Secondly, the deviation of the observed photoionization process characteristics from that calculated in a single-electron approximation is direct measure of *interelectron correlations* in atoms and ions. Thirdly, it is of interest to assess the abilities of existing theoretical methods to predict results prior to the corresponding experimental measurement. This paper applies the random

phase approximation with exchange (RPAE) to calculations of the isoelectronic series C^-, N, O^+ photoionization cross-section and angular anizotropy parameters. Choosing targets with the same electronic configuration enables to clarify the role of the competition between the interelectron which leads to correlations and the nuclear charge which determines the independent motion. The comparison of the results for these objects will demonstrate whether it is possible to interpolate or extrapolate data to the nearest neighbor.

2 METHOD OF CALCULATION

The objects C^-, N and O^+ have in their ground states a semi-filled $2p^3$-subshell. According to Hund rule all these electrons have the same projection of spin which for consistency is considered to be directed "up" and is denoted by an arrow $\uparrow$. Then, due to presence of exchange only between electrons with the same spin projections each subshell is split into two levels with opposite spin directions: "up" and "down" levels. As a result the electron configuration of the objects under consideration can be presented as

$$1s^1 \uparrow 1s^1 \downarrow 2s^1 \uparrow 2s^1 \downarrow 2p^3 \uparrow \tag{1}$$

To calculate the photoionization cross-section for an atom or ion with such a configuration of electrons the spin-polarized version of the RPAE is used in this paper (Amusia and Ivanov, 1987; Amusia, 1990). This version treats "up" and "down" electrons as different particles without exchange between them. Therefore, the RPAE scheme can be applied straightforwardly in a version which takes into account the existence of two kinds of different particles. The separation into "up" and "down" electrons is required in order to have only closed levels for each of them, namely, $1s2s2p \uparrow$ and $1s2s \downarrow$. This makes the ground state (1) non-degenerate. The non-degeneracy of the ground state considerably simplifies the application of many-body theory approaches including RPAE. In fact, the separation into "up" and "down" electrons is an approximation which treats total spin projection as a precise quantum number instead of the total spin itself. However, special estimates demonstrate that the inaccuracy introduced by this approximation is quite small.

From the physical point of view RPAE is a mehtod in which the total photoionization amplitude $\langle f|D(\omega)|i\rangle$ describing the electron transition from the initial $|i\rangle$ to the final state $\langle f|$ after absorbing a photon with frequency ω is presented as a sum of two terms, the direct one $\langle f|\hat{d}|i\rangle$ and the indirect $\langle f|\Delta D|i\rangle$ vie the virtual excitation of all atomic electrons except ionized one i. The first term represents the contribution to the amplitude in a single-electron approximation while second accounts for correlations. In RPAE the correction ΔD is determind by solving an integral equation which symbolically, in the operator form, can be presented as (Amusia, 1990):

$$\hat{D}(\omega) = \hat{d} + \hat{U}\chi(\omega)\hat{D}(\omega), \tag{2}$$

where U is the combination of the direct and exchange Coulomb interelectron interaction and $\chi(\omega)$ accounts for the excitation both virtual and real of all single electron–single vacancy pairs. From equation (2) one has in RPAE $\Delta D = \hat{U}\chi(\omega)\hat{D}$.

For the two-component systems under consideration equation (2) can be presented in 2 × 2 matrix form (Amusia, 1990):

$$\begin{pmatrix} \hat{D}_\uparrow(\omega) \\ \hat{D}_\downarrow(\omega) \end{pmatrix} = \begin{pmatrix} \hat{d}_\uparrow \\ \hat{d}_\downarrow \end{pmatrix} + \begin{pmatrix} U_{\uparrow\uparrow} & V_{\uparrow\downarrow} \\ V_{\downarrow\uparrow} & U_{\downarrow\downarrow} \end{pmatrix} \begin{pmatrix} \chi_{\uparrow\uparrow}(\omega) & 0 \\ 0 & \chi_{\downarrow\downarrow}(\omega) \end{pmatrix} \begin{pmatrix} \hat{D}_\uparrow(\omega) \\ \hat{D}_\downarrow(\omega) \end{pmatrix}. \quad (3)$$

Here, it is taken into account that "up" and "down" electrons can not change their identity under the action of the incoming photon which is unable to alter the electron spin. Therefore, the amplitudes $\hat{D}(\omega)$ (or $\hat{d}$) are either "up" or "down". As to the interelectron interaction, its inclusion permits us to take into account not only the diagonal terms ($\uparrow\uparrow$ or $\downarrow\downarrow$) but also the mutual influence of the "up" and "down" channels. Virtual electron excitations by a photon are spinless and therefore their contribution to equation (3) is diagonal, i.e. either $\uparrow\uparrow$ or $\downarrow\downarrow$. Spin-orbit interaction is negleted in equation (3), and absorbtion of only dipole photons is considered.

The photoionization cross-section is propotional to $|D(\omega)|^2$. The total and differential cross-sections are sums of "up" and "down" contributions. Analytical expression corresponding to the symbolic equation (3) has the following form:

$$\begin{aligned} (\varepsilon l\uparrow|D(\omega)|i\uparrow) &= (\varepsilon l\uparrow|d|i\uparrow) + \sum_{\varepsilon' l'>F, i'\le F} \{(\varepsilon' l'\uparrow|D(\omega)|i'\uparrow)(\omega-\varepsilon'-I_{i'\uparrow})^{-1} \\ &\times (\varepsilon' l'\uparrow, i\uparrow|U|i'\uparrow, \varepsilon l\uparrow) + (i'\uparrow|D(\omega)|\varepsilon' l'\uparrow)(\omega+\varepsilon'+I_{i'\uparrow})^{-1} \\ &\times (i'\uparrow, i\uparrow|U|\varepsilon' l'\uparrow, \varepsilon l\uparrow) + (\varepsilon' l'\downarrow|D(\omega)|i'\downarrow)(\omega-\varepsilon'-I_{i'\downarrow})^{-1} \\ &\times (\varepsilon' l'\downarrow, i\uparrow|V|i'\downarrow, \varepsilon l\uparrow) + (i'\downarrow|D(\omega)|\varepsilon' l'\downarrow)(\omega+\varepsilon'+I_{i'\downarrow})^{=1} \\ &\times (i'\downarrow i\uparrow|V|\varepsilon' l'\downarrow, \varepsilon l\uparrow)\}. \end{aligned} \quad (4)$$

where summation (integration) is performed over all vacant εl ($> F$) and occupied $i \equiv n_i l_i$ ($\le F$) states with n_i being the principal quantum number and l_i the angular momentum of the occupied electron states. In the εl combination ε is the electron energy and l is the angular momentum $I_{i'\updownarrow}$. The ionization potential of the occupied levels $i' \updownarrow U$ includes direct interaction and negative contribution of the exchange term

$$(\varepsilon' l'\uparrow, i\uparrow|U|i'\uparrow, \varepsilon l\uparrow) = (\varepsilon' l'\uparrow, i\uparrow|V|i'\uparrow, \varepsilon l\uparrow) - (\varepsilon' l'\uparrow, i\uparrow|V|\varepsilon l\uparrow, i'\uparrow). \quad (5)$$

A similar equation determins the spin-down $(\varepsilon l\downarrow|D(\omega)|i\downarrow)$ matrix element. The excited electron state $|\varepsilon l)$, $|\varepsilon' l')$ and that occupied in the target atom $|i)$, $|i')$ are represented by wave functions – solutions of the spin-polarized version of the Hartree–Fock (SPHF) equations. These are generalized versions of the usual HF equations for the systems with two kinds of the different "up" and "down" particles without any exchange between them.

After separating the single-electron wavefunction into radial and angular parts and performing the integration over the angular variables analytically an alternative equation is obtained to equation (4) for the reduced matrix elements $(\varepsilon l\uparrow\|D(\omega)\|n_i l_i\uparrow)$ or $(\varepsilon l\downarrow\|D(\omega)\|n_i l_i\downarrow)$. Because the photon is a dipole one has

$l = l_i \pm 1$. Using these matrix elements the photoionization cross-section of a channel is expressed as†:

$$\sigma_{n_i l_i \updownarrow}(\omega) = \frac{8\pi^2\omega}{3c}\{|[\varepsilon l_i + 1, \updownarrow \|D(\omega)\|n_i l_i, \updownarrow|^2 + |(\varepsilon l_i - 1, \updownarrow \|D(\omega)\|n_i l_i, \updownarrow|^2\} \quad (6)$$

$$\frac{d\sigma_{n_i l_i \updownarrow}(\omega)}{d\Omega} = \frac{\sigma_{n_i l_i \updownarrow}(\omega)}{4\pi}[1 + \beta_{n_i l_i \updownarrow}(\omega) P_2(\cos\theta)], \quad (7)$$

c being the speed of light. The angular anisotropy parameter $\beta_{n_i l_i \updownarrow}(\omega)$ is determined by the following expression:

$$\begin{aligned}\beta_{n_i l_i \updownarrow}(\omega) &= \{(2l_i + 1)(|D_{l_i+1,\updownarrow}(\omega)|^2 + |D_{l_i-1,\updownarrow}(\omega)|^2)\}^{-1} \\ &\times \{(2l_i + 2)|D_{l_i+1,\updownarrow}(\omega)|^2 + (l_i - 1)|D_{l_i-1,\updownarrow}(\omega)|^2 \\ &+ 6\sqrt{l_i(l_i+1)}\Re[D_{l_i+1,\updownarrow}(\omega)\, D^*_{l_i-1,\updownarrow}(\omega)\, e^{i\delta_{l_i+1,\updownarrow}(\varepsilon) - \delta_{l_i-1,\updownarrow}(\varepsilon)}]\} \quad (8)\end{aligned}$$

$$\varepsilon = \omega - I_i, \quad [\varepsilon l \uparrow \|D(\omega)\|n_i l_i \uparrow].$$

In equation (8) $\delta_{l_i \pm 1,\updownarrow}(\varepsilon)$ are the photoelectron elastic scattering phase shifts.

The SPHF and SPRPAE equations are solved numerically using the program ATOM (Amusia and Chernysheva, 1983; Chernysheva *et al.*, 1993). The integration over ε' is approximated by summation; the infinite sums over discrete excited states and the continuous spectrum are truncated to three to five discrete levels and 20–35 points in the continuous spectrum. The accuracy of the numerical procedure is checked by performing calculations with two forms of the dipole photon-electron interaction operator – "length" r and "velocity" $1/\omega c\ \nabla$. These two forms must lead to the same results for the cross-section not only if the precise atomic wavefunctions are used but also in the RPAE frame. This statement is correct if the pure numerical procedure of solving HF and RPAE equations is accurate enough and these equations are applied to objects with really non-degenerate ground states. Even for really non-degenerate ground states to guarantee the equivalence of the r and ∇ results the summation in equation (4) must be performed over all occupied states including $1s\ \updownarrow$. In this paper the contribution of $1s$-electrons is completely neglected. Therefore, additional sources of inaccuracy, namely, the increase in the difference between r and ∇ results are expected at high ω comparable to $\omega \cong I_{1s}$. Owing to the dipole nature of the absorbed photon the following transitions take place from $2s \uparrow 2s \downarrow 2p^3 \uparrow$ levels: $2s \uparrow \Rightarrow n, \varepsilon p \uparrow$; $2s \downarrow \Rightarrow n, \varepsilon p \downarrow$, $2p^3 \uparrow \Rightarrow 2p^2 n, \varepsilon d \uparrow$, $2p^3 \uparrow \Rightarrow 2p^2 n, \varepsilon s \uparrow$. All these are included in the sum over i' and $\varepsilon' l'$. The mutual influence of these transitions is taken into account by solving equation (4).

When a discrete excitation of an inner level is above the ionization threshold of an outer level, the former is autoionizing. The process of autoionization leads to fast and very specific variation of the photoionization cross-section which is called a Fano-profile. The formation of Fano-profiles is described by equation (4) and is included in our calculations.

†The atomic system of units is used in this paper: $e = m_e = \hbar = 1$, e and m_e being the electron charge and mass, respectively.

Table 1. Oscillator strengths (OS) for N and O^+

Atom	*Transition*	*Energy of excitation (Ry)*	*OS*		
			SPHF, l-form	*SPHF, v-form*	*SPRPAE*
N	$2s\downarrow \Rightarrow 2p\downarrow$	0.722	0.58	0.60	0.29
	$2p\uparrow \Rightarrow 3s\uparrow$	0.835	0.12	0.11	0.088
	$2p\uparrow \Rightarrow 4s\uparrow$	1.017	0.02	0.18	0.028
	$2p\uparrow \Rightarrow 5s\uparrow$	1.074	0.007	0.007	0.011
	$2p\uparrow \Rightarrow 3d\uparrow$	1.028	0.069	0.056	0.068
	$2p\uparrow \Rightarrow 4d\uparrow$	1.078	0.035	0.028	0.033
	$2p\uparrow \Rightarrow 5d\uparrow$	1.1012	0.019	0.05	0.02
O^+	$2s\downarrow \Rightarrow 2p\downarrow$	1.028	0.48	0.5	0.28
	$2s\downarrow \Rightarrow 3p\downarrow$	2.43	0.026	0.025	0.035
	$2s\downarrow \Rightarrow 4p\downarrow$	2.74	0.011	0.01	0.017
	$2s\uparrow \Rightarrow 2p\uparrow$	3.46	0.047	0.042	0.0055
	$2p\uparrow \Rightarrow 3d\uparrow$	2.2	0.356	0.297	0.38
	$2p\uparrow \Rightarrow 4d\uparrow$	2.4	0.154	0.127	0.18
	$2p\uparrow \Rightarrow 5d\uparrow$	2.5	0.078	0.064	0.07
	$2p\downarrow \Rightarrow 3s\uparrow$	1.77	0.12	0.11	0.14

The wavefunctions of electrons in their excited ε and occupied i states and the elastic scattering phase shifts for photoelectrons $\delta_l(\varepsilon)$ are also obtained. By calculating the matrix elements $(\varepsilon l\|D(\omega)\|i)$ for $\varepsilon = \omega - I_i$ and the phase shifts $\delta_l(\varepsilon)$ it becomes possible to determine the cross-section equation (6), angular distribution equations (7) and (8) the spin polarization of the photoelectron (Cherepkov, 1983), i.e. to determine purely theoretically all chracteristics of the photoionization process.

3 RESULTS OF CALCULATIONS

In Figures 1–15 the results of calculations for partial and total photoionization cross-section and angular anizotropy parameters are presented. In Table 1 the N and O^+ oscillator strenghts are given.

In C^- the $2p\uparrow$ cross-section is large as can be seen in Figures 1 and 2, with $2p \Rightarrow \varepsilon d$ and $2p \Rightarrow \varepsilon s$ transition contributions. While the first increases rather slowly in the SPHF reaching its maximum of about 20 Mb at 0.6 Ry which is quite far from the threshold (0.156 Ry), the second jumps just at the threshold, its maximum being about 6 Mb. The difference between length and velocity forms is quite large. The SPHF $2s\updownarrow$ cross-sections are unexpectedly large (Figures 3 and 4), up to 45 Mb for $2s \Rightarrow \varepsilon p\downarrow$ and look like discrete exitations with a width of about 0.2 Ry for $2s \Rightarrow \varepsilon p\uparrow$ and 0.1 Ry for $2s \Rightarrow \varepsilon p\downarrow$. The SPRPAE calculations modify the results considerably. The $2p \Rightarrow \varepsilon d\uparrow$ cross-section acquires a region with a very rapid variation (see Figure 1) which looks like a Fano-profile because a narrow continuous spectrum maximum in the $2s \Rightarrow \varepsilon p\downarrow$ channel acts as a discrete excitation embedded into the $2p \Rightarrow \varepsilon d, s$ continuous spectrum, just as previously demonstrated for Si^-

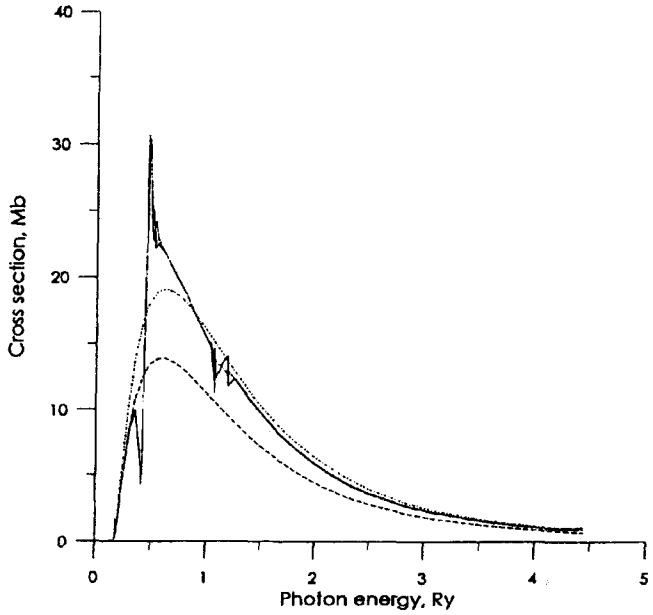

Figure 1 Cross-sections of C^-. SPHF calculations of the $2p \Rightarrow \epsilon d$ up channel: -·-, length form; ---, velocity form, SPRPAE calculations of the $2p \Rightarrow \epsilon d$ up channel with four-channel interaction: . . ., length form; —, velocity form.

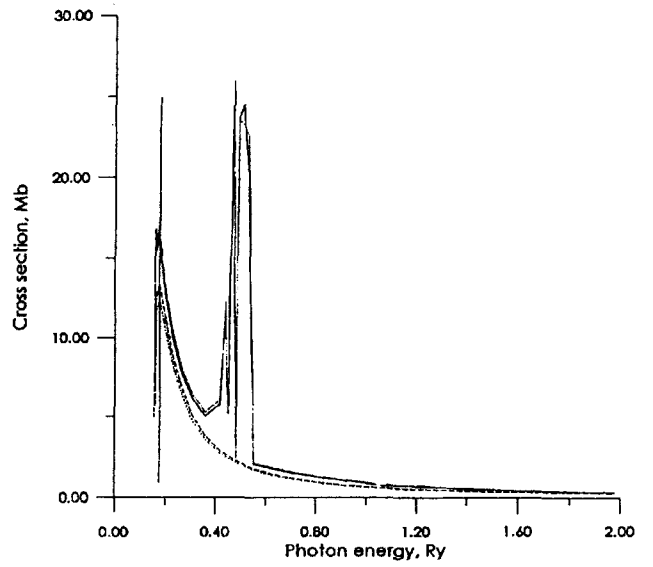

Figure 2 Cross-sections of C^-. SPHF calculations of the $2p \Rightarrow \epsilon s$ up channel: -·-, length form; ---, velocity form, SPRPAE calculations of the $2p \Rightarrow \epsilon s$ up channel with four-channel interaction: . . ., length form; —,velocity form.

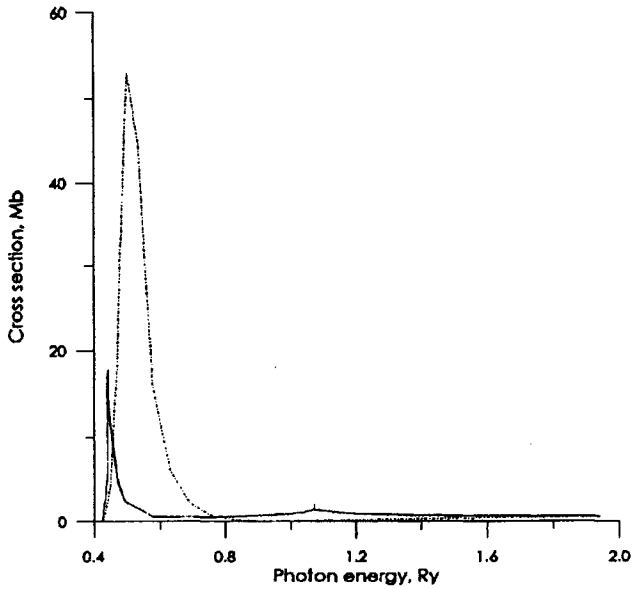

Figure 3 Cross-sections of C^-. SPHF calculations of the $2s \Rightarrow \epsilon p$ down channel: ---, length form; ---, velocity form, SPRPAE calculations of the $2s \Rightarrow \epsilon p$ down channel with four-channel interaction: . . ., length form; —, velocity form.

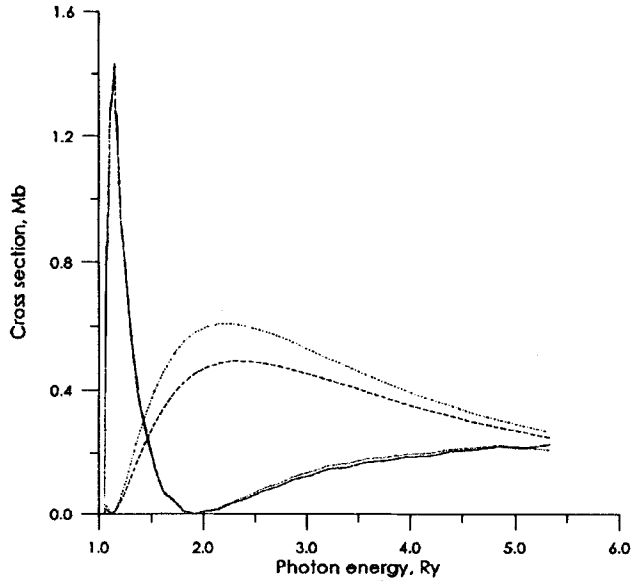

Figure 4 Cross-sections of C^-. SPHF calculations of the $2s \Rightarrow \epsilon p$ up channel: ---, length form; ---, velocity form, SPRPAE calculations of the $2s \Rightarrow \epsilon p$ up channel with four-channel interaction: . . ., length form; —, velocity form.

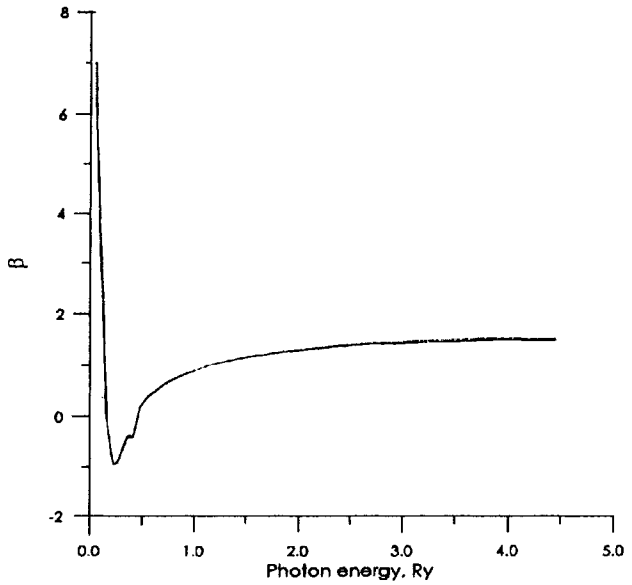

Figure 5 Asymmetry parameter of the $2p^3 \uparrow$ channel in C^-. SPRPAE calculations with four-channel interaction: ..., length form; —, velocity form.

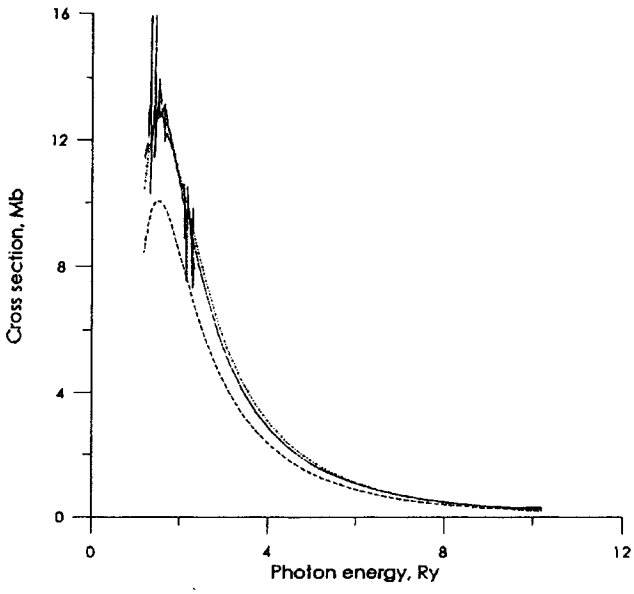

Figure 6 Cross-sections of N. SPHF calculations of the $2p \Rightarrow \epsilon d$ up channel: ---, length form; ---, velocity form, SPRPAE calculations of the $2p \Rightarrow \epsilon d$ up channel with four-channel interaction: ..., length form; —, velocity form.

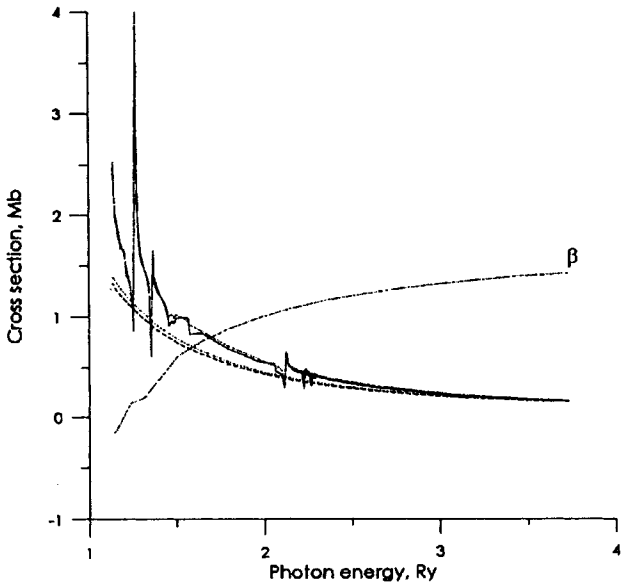

Figure 7 Cross-section of N. SPHF calculations of the $2p \Rightarrow \varepsilon s$ up channel: ---, length form; ---, velocity form, SPRPAE calculations of the $2p \Rightarrow \varepsilon s$ up channel with four-channel interaction: . . ., length form; —, velocity form.

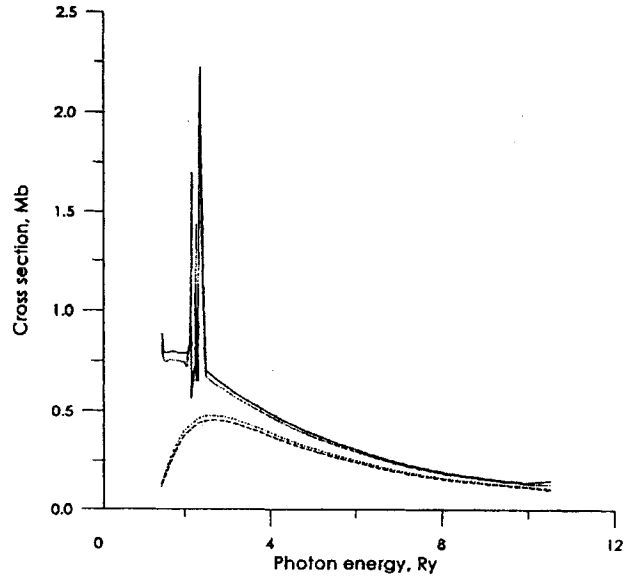

Figure 8 Cross-sections of N. SPHF calculations of the $2s \Rightarrow \varepsilon p$ down channel: ---, length form; ---, velocity form, SPRPAE calculations of the $2s \Rightarrow \varepsilon p$ down channel with four-channel interections: . . ., length form; —, velocity form.

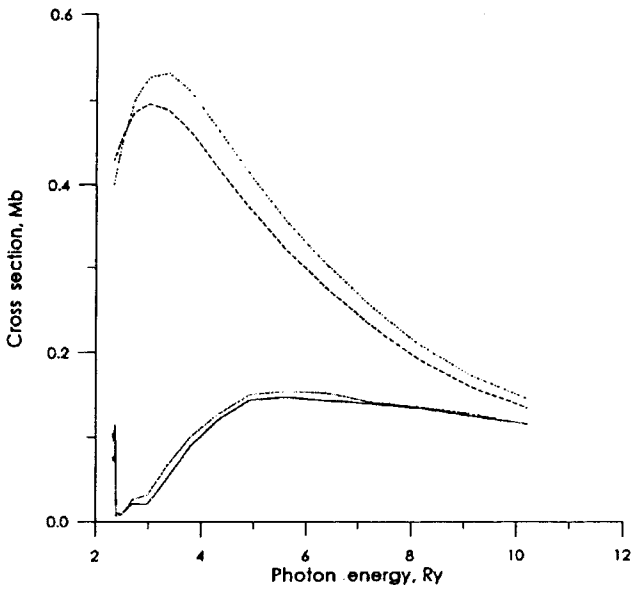

Figure 9 Cross-sections of N. SPHF calculations of the $2s \Rightarrow \varepsilon p$ up channel: ---, length form; ---, velocity form, SPRPAE calculations of the $2s \Rightarrow \varepsilon p$ up channel with four-channel interaction: . . ., length form; —, velocity form.

(Amusia *et al.*, 1986; Amusia, 1990). The $2s \Rightarrow \varepsilon p \uparrow$ cross-section loses about 90 percent at its strength (Figure 3). The $2p \Rightarrow \varepsilon s$ channel is also strongly affected by the $2s \Rightarrow \varepsilon p \downarrow$ resonance acquiring an additional maximum at 0.425 Ry (see Figure 2). Of particular interest is the angular anizotropy parameter $\beta(\omega)$ for $2p$-electrons in C^-, which is strongly influenced by the $2p^3 \uparrow$ and $2s \downarrow$ electron correlations accounted for by the SPRPAE. In the frequency region considered (see Figure 5) $\beta_{2p\uparrow}(\omega)$ is a rapidly varying function whith autoionizational structure at $\omega = 0.2$-0.5 Ry.

In general, the results obtained for C^- are in agreement with those presented by (Gribakin *et al.*, 1992). However, there are some differences. For instance, the cross-section of the $2s \Rightarrow \varepsilon p \uparrow$ channel is considerably bigger here. This can be attributed to inclusion of all the interactions in the four channels simultaneously which was not done by Gribakin *et al.* (1992). Note, that references to previous publications on C^- photoionization cross-section calculations using other methods as well as experimental data can be found in Gribakin *et al.* (1992).

The situation in N differs considerably from that in C^-. Both the $2p \Rightarrow \varepsilon d$ and $2p \Rightarrow \varepsilon s$ transitions have their maxima at the threshold (see Figures 6 and 7), but the $2p \Rightarrow \varepsilon d$ contribution is bigger by a factor of 5. The narrow continuum spectrum resonances of $2s \Rightarrow \varepsilon p \updownarrow$ in C^- are absent in N. The influence of SPRPAE corrections in the $2p \Rightarrow \varepsilon p$ transition is small, almost completely eliminating the "length" and "velocity" difference (see Figures 6 and 7). The $2s \Rightarrow \varepsilon p \updownarrow$ cross-sections are small as seen in Figures 8 and 9. It is of interest that the effect

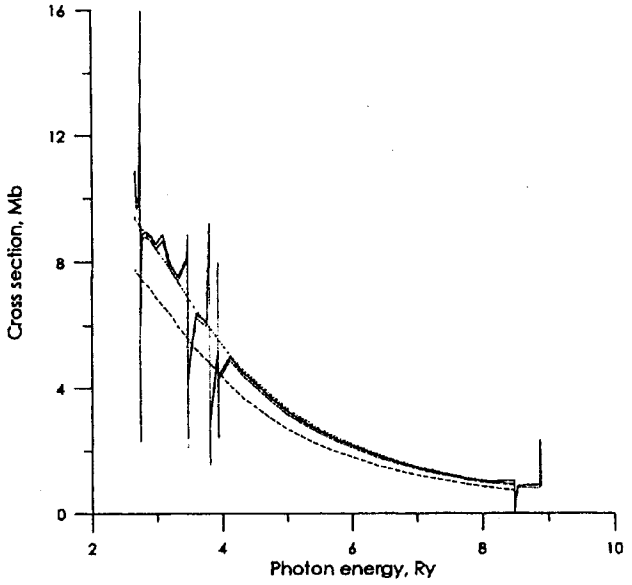

Figure 10 Cross-sections of O^+. SPHF calculations of the $2p \Rightarrow \epsilon d$ up channel: ---, length form; ---, velocity form, SPRPAE calculations of the $2p \Rightarrow \epsilon d$ up channel with four-channel interaction: ..., length form; —, velocity form.

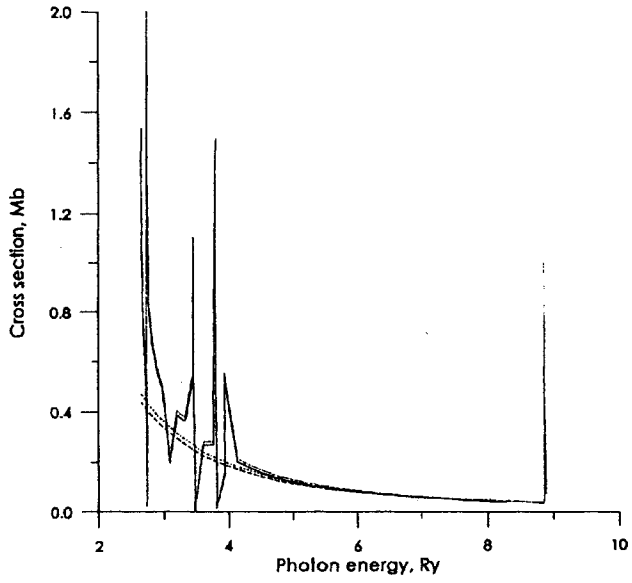

Figure 11 Cross-sections of O^+. SPHF calculations of the $2p \Rightarrow \epsilon s$ up channel: ---, length form; ---, velocity form, SPRPAE calculations of the $2p \Rightarrow \epsilon s$ up channel with four-channel interaction: ..., length form; —, velocity form.

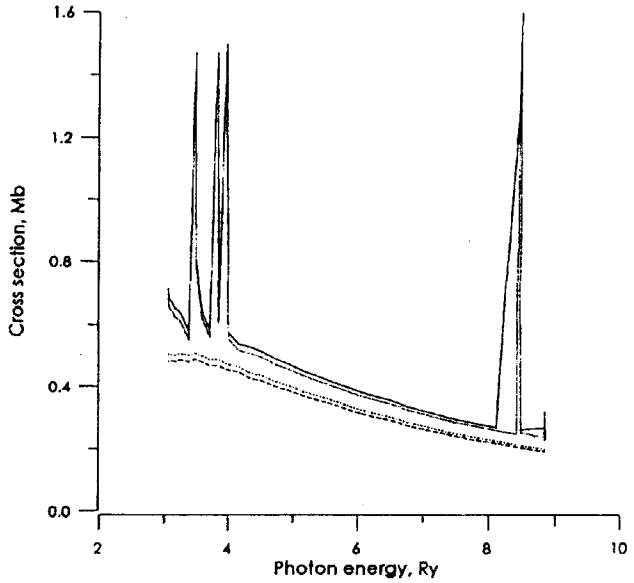

Figure 12 Cross-sections of the O^+. SPHF calculations of the $2s \Rightarrow \varepsilon p$ down channel: ---, length form; ---, velocity form, SPRPAE calculations of the $2s \Rightarrow \varepsilon p$ down channel with four-channel interaction: . . ., length form; —, velocity form.

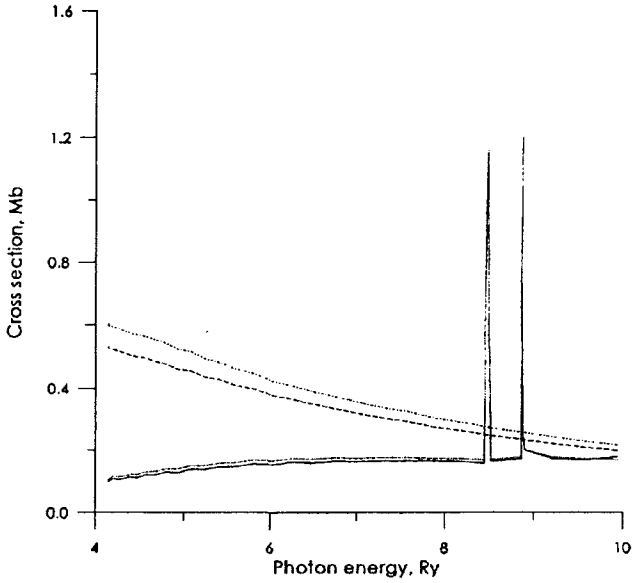

Figure 13 Cross-sections of O^+. SPHF calculations of the $2s \Rightarrow \varepsilon p$ up channel: ---, lengh form; ---, velocity form, SPRPAE calculations of the $2s \Rightarrow \varepsilon p$ up channel with four–channel interaction: . . ., length form; —, velocity form.

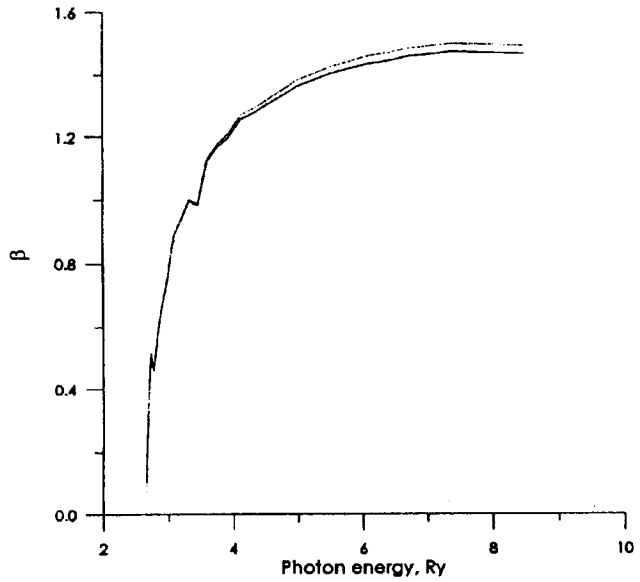

Figure 14 Asymmetry parameter of the $2p^3$ ↑ channel in O^+. SPRPAE calculations with four-channel interaction: ..., length form; —, velocity form.

of the outer $2p^3$-electrons upon the $2s$-photoionization cross-section is opposite for the $2s \Rightarrow \varepsilon p \downarrow$ and $2s \Rightarrow \varepsilon p \uparrow$ transitions. In the first case the SPRPAE value is bigger while in the second it is much smaller than that in the HF approximation. The angular anizotropy parameter depicted in Figure 10 is not particularly interesting: it is a smooth function growing from zero at the threshold up to 1.5 well above it. Recently, SPRPAE calculations for N were performed by Ivanov and Chernysheva (1990). This reference includes experimental data and references to previous calculations. In general there is agreement between the presented results and these of Ivanov and Chernysheva (1990). The main difference is in accounting for all transitions simultaneously whithin the SPRPAE frame which is achieved in this paper for first time leading to an almost complete coincidance between length and velocity SPRPAE results.

The SPHF $2p \Rightarrow \varepsilon d \uparrow$ cross-section for O^+ is smaller than for N, its maximum value being only about 8 Mb as seen in Figure 10. The $2p \Rightarrow \varepsilon s \uparrow$ SPHF contribution is, according to Figure 11, very small, less than 0.4 Mb. The SPRPAE corrections qualitatively modify the cross-section of $2p \uparrow$-electrons just near the threshold: a number of narrow resonances due to discrete excitations of $2s$-electrons appear. Alterations above the region of the minimum and maximum are small. As seen in Figures 12 and 13, only the $2s \Rightarrow \varepsilon p \uparrow$ channel is strongly affected with the SPRPAE method: the corresponding correction becomes considerably smaller as in the N case. The changes in $2s \Rightarrow \varepsilon p \downarrow$ cross-section are much less impressive. Near the threshold region, the angular anizotropy parameter is strongly affected by the

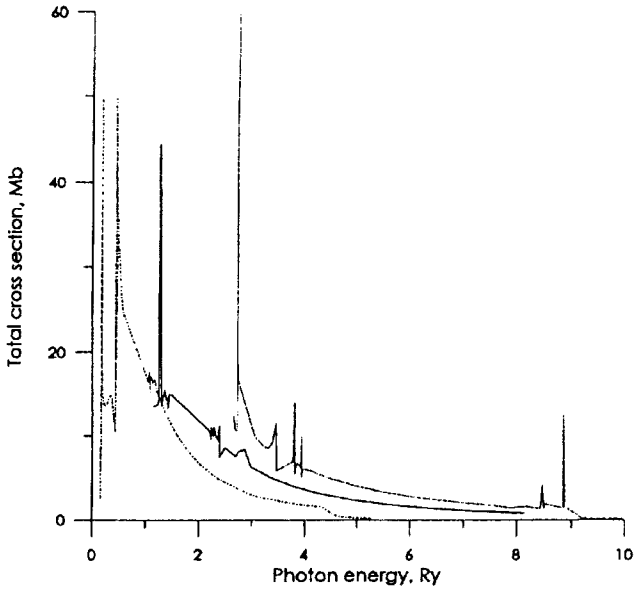

Figure 15 Total cross-sections. SPRPAE calculations with four-shannel interaction, length form: ---, C^-; —, N; . . ., O^+.

SPRPAE corrections At higher frequences it is a smooth function of ω (see Figure 14). Within the HF frame the tendency with the growth of the nuclear charge is simple: the cross-section maximum is shifted towards the threshold, finally transferring a bigger and bigger fraction of its total intensity to the discrete excitations. After inclusion of SPRPAE effects the situation becomes much more complicated and irregular. The variations for $2s \rightarrow \varepsilon p \updownarrow$ channels is extremely strong from C^- to N and is much smaller at the next step from N to O^+. Without doubt, other characteristics of the photoionization process, such as spin orientation of the photoelectron are also strongly affected by the SPRPAE corrections.

4 CONCLUDING REMARKS

For a very long period of time the hydrogenic approximation was the only tool to estimate and even to calculate the photoionization cross-section. The results obtained (see Figure 15) were smooth functions of the nuclear charge. It formed the basis of different extra- and interpolation procedures used in order to avoid complicated calculations. The results presented above for isoelectronic series of comparatively simple ions and atoms manifest clear irregularities which occur in cross-sections and angular anizotropy parameters with the growth of nuclear charge by the smallest possible step. On the other hand, progress in computation techniques and development of the software permits us to perform extensive and quite accurate calculations

comparatively simply and with reasonable amount of effort. The final aim is to develop RPAE calculations to a level at which they will be as simple to apply as hydrogenic calculations, thus forming the basis of a new initial approximation. The difference between RPAE results and experimental data demonstrate that further improvement in the theory of many-electron atom photoionization are neccesary.

Acknowledgment

We would like to acknowledge helpful discussions with Professor V. K. Ivanov.

This work is funded by the International Science and Technlogy Center (ISTC) under the Project No. 076–95.

References

Amusia, M. Ya.(1990) *Atomic Photoeffect*, Plenum Press, New York, London.

Amusia, M. Ya. and Chernysheva, L. V. (1983) *ATOM-Computation of Atomic Structure*, Leningrad, Nauka (in Russian).

Amusia, M. Ya., Gribakin, G. F., Ivanov, V. K., and Chernysheva, L. V. (1986) *Isv. Akad. Nauk Ser. Fiz.* **50**, 1274–1278; and (1990) *J. Phys. B* **23**, 385–91.

Amusia, M. Ya. and Ivanov, V. K. (1987) *Sov. Phys. Usp.* **152**, 185.

Cherepkov, N. A. (1983) *Adv. At. Mol. Phys.* **19**, 395–447.

Chernysheva, L. V., Semenov, S. K., and Cherepkov, N. A. (1993) *Preprint PTI-1620*, St. Petersburg.

Gribakin, G. F., Gribakina, A. A., Gul'tsev, B. V., and Ivanov, V. K. (1992) *J. Phys. B.* **25**, 1757–1772.

Ivanov, V. K. and Chernysheva, L. V. (1990) *Opt. Spectrosc.* **69**, 289–294.